University Library

MINERVA ACCESS

A gateway to Melbourne's research publications

Minerva Access is the Institutional Repository of The University of Melbourne

Author/s:
Palmer, JG;Cook, ER;Turney, CSM;Allen, K;Fenwick, P;Cook, BI;O'Donnell, A;Lough, J;Grierson, P;Baker, P

Title:
Drought variability in the eastern Australia and New Zealand summer drought atlas (ANZDA, CE 1500-2012) modulated by the Interdecadal Pacific Oscillation

Date:
2015-11-23

Citation:
Palmer, J. G., Cook, E. R., Turney, C. S. M., Allen, K., Fenwick, P., Cook, B. I., O'Donnell, A., Lough, J., Grierson, P. & Baker, P. (2015). Drought variability in the eastern Australia and New Zealand summer drought atlas (ANZDA, CE 1500-2012) modulated by the Interdecadal Pacific Oscillation. Environmental Research Letters, 10 (12), https://doi.org/10.1088/1748-9326/10/12/124002.

Persistent Link:
https://hdl.handle.net/11343/116476

License:
CC BY

IOPscience iopscience.iop.org

Home Search Collections Journals About Contact us My IOPscience

Drought variability in the eastern Australia and New Zealand summer drought atlas (ANZDA, CE 1500–2012) modulated by the Interdecadal Pacific Oscillation

This content has been downloaded from IOPscience. Please scroll down to see the full text.

2015 Environ. Res. Lett. 10 124002

(http://iopscience.iop.org/1748-9326/10/12/124002)

View the table of contents for this issue, or go to the journal homepage for more

Download details:

IP Address: 128.250.4.115
This content was downloaded on 16/02/2016 at 03:38

Please note that terms and conditions apply.

Environmental Research Letters

LETTER

Drought variability in the eastern Australia and New Zealand summer drought atlas (ANZDA, CE 1500–2012) modulated by the Interdecadal Pacific Oscillation

Jonathan G Palmer[1], **Edward R Cook**[2], **Chris S M Turney**[1], **Kathy Allen**[3], **Pavla Fenwick**[4], **Benjamin I Cook**[2,5], **Alison O'Donnell**[6], **Janice Lough**[7], **Pauline Grierson**[6] **and Patrick Baker**[3]

[1] Climate Change Research Centre, School of Biological, Earth and Environmental Sciences, University of New South Wales, Sydney, NSW 2015, Australia
[2] Lamont-Doherty Earth Observatory of Columbia University, Palisades, NY 10964, USA
[3] School of Ecosystem and Forest Sciences, University of Melbourne, Richmond, Victoria, 3121, Australia
[4] Gondwana Tree-ring Laboratory, P O Box 14, Little River, Canterbury, 7546, New Zealand
[5] NASA Goddard Institute for Space Studies, 2880 Broadway, New York, NY 10025, USA
[6] Ecosystems Research Group, School of Plant Biology, The University of Western Australia, Crawley, WA 2016, Australia
[7] Australian Institute of Marine Science, PMB 3, Townsville MC, Townsville, QLD 4810, Australia

E-mail: j.palmer@unsw.edu.au

Keywords: gridded summer drought atlas, eastern Australia, palaeoclimatology, Interdecadal Pacific Oscillation (IPO), multi-decadal hydroclimate variability

Supplementary material for this article is available online

OPEN ACCESS

RECEIVED
30 September 2015

REVISED
30 October 2015

ACCEPTED FOR PUBLICATION
3 November 2015

PUBLISHED
23 November 2015

Content from this work may be used under the terms of the Creative Commons Attribution 3.0 licence.

Any further distribution of this work must maintain attribution to the author(s) and the title of the work, journal citation and DOI.

Abstract

Agricultural production across eastern Australia and New Zealand is highly vulnerable to drought, but there is a dearth of observational drought information prior to CE 1850. Using a comprehensive network of 176 drought-sensitive tree-ring chronologies and one coral series, we report the first Southern Hemisphere gridded drought atlas extending back to CE 1500. The austral summer (December–February) Palmer drought sensitivity index reconstruction accurately reproduces historically documented drought events associated with the first European settlement of Australia in CE 1788, and the leading principal component explains over 50% of the underlying variance. This leading mode of variability is strongly related to the Interdecadal Pacific Oscillation tripole index (IPO), with a strong and robust antiphase correlation between (1) eastern Australia and the New Zealand North Island and (2) the South Island. Reported positive, negative, and neutral phases of the IPO are consistently reconstructed by the drought atlas although the relationship since CE 1976 appears to have weakened.

1. Introduction

Knowledge of natural long-term hydroclimatic variability is essential for water-resource and land-use management and to manage risks associated with extreme events such as drought (Bell *et al* 2013). However, there is a dearth of reliable high-resolution (temporal and spatial) records of past rainfall patterns prior to the late 19th century in Australia and New Zealand and for much of the Southern Hemisphere (SH), which limits our ability to estimate long-term hydroclimatic variability. This lack of long-term hydroclimate data poses great challenges for managing water resources, which have been largely focused on short-term response rather than proactive planning and mitigation strategies (Ding *et al* 2011). Droughts in Australia and New Zealand can have significant ecological, social and economic impacts. For example, the 2002 to 2003 Australian drought caused an overall reduction of gross domestic production (GDP) by 1.6% (Horridge *et al* 2005) and was associated with severe bushfires across New South Wales and the Australian Capital Territory. The 2013 drought in New Zealand was estimated to have caused GDP to fall by 0.6% (McDonald 2013). There is thus an urgent need to quantify and improve understanding of past

© 2015 IOP Publishing Ltd

natural climatic variations, through accurate, quantified, and absolutely-dated reconstructions that capture variation over annual, decadal and multi-decadal timescales, which in turn can be used to test and refine global climate models.

Here we report the development of an eastern Australia and New Zealand Drought Atlas (ANZDA), a seasonally resolved gridded spatial reconstruction of drought and wet periods over the past 500 years, derived from a network of 176 tree-ring chronologies from both countries and Indonesia as well as a coral record from Queensland (177 records in total). The region in general was chosen due to common climate influences linked to droughts—predominantly the interdecadal Pacific oscillation (IPO, Power *et al* 1998) and El Niño-Southern oscillation (ENSO) events (Kiem *et al* 2003). The ANZDA aims to provide spatio-temporal details of known historical Australian and New Zealand drought events and to reveal the occurrence, severity, and fingerprint of previously unknown droughts, with their close linkages to large-scale patterns of tropical Pacific sea surface temperatures (SST). The ANZDA will thus provide a long-term context for recent drought variability that informs climate modelling, prediction and attribution.

2. Data and methods

Australia and New Zealand are fortunate to have a range of long-lived tree species with clear annual rings (Enright and Ogden 1995). This has enabled annual growth patterns to be matched (crossdated) between different trees to produce a year-by-year account of past environmental conditions (i.e. dendroclimatology). Since the pioneering regional tree-ring studies of LaMarche *et al* (1979) more than 150 tree-ring chronologies have been developed from over a dozen different tree species in Australia and New Zealand with most of the data archived at the International Tree-ring Data Bank (ITRDB; www.ncdc.noaa.gov/data-access/paleoclimatology-data/datasets/tree-ring). For Australia there has traditionally been a strong bias towards Tasmanian conifers but this situation has changed recently with successful crossdating of other species on the mainland (e.g. Cullen and Grierson 2009, McDougall *et al* 2012, Heinrich and Allen 2013, O'Donnell *et al* 2015). In this study, 176 tree-ring chronologies were drawn from the ITRDB repository or other unpublished tree-ring data archives from current research programs of the authors plus a hydroclimatically sensitive coral luminescence record from the Great Barrier Reef (table S1; figure 1). We used 94 tree-ring series from New Zealand, 68 from Tasmania, three from the Northern Territory, nine from Indonesia and two from Western Australia; a network broadly encircling the eastern Australian region.

The tree-ring measurement series used in the chronologies were screened for dating problems prior to chronology development using the software program COFECHA (Holmes 1983, Grissino-Mayer 2001). This meant some individual series were truncated, or more rarely deleted, because of obvious statistical signs of poor crossdating. Most of the detected problems arose because the series had been collected before recent advances in quality control (e.g. COFECHA, Holmes 1983, Grissino-Mayer 2001) had become available and widely adopted. For the remaining series, the quality of the data had been checked by contributing authors using now standard quality-control procedures (see supporting information for further details). After the data were screened for quality and correct dating, the tree-ring chronologies were developed using the 'signal free' method of tree-ring standardization (Melvin and Briffa 2008), which minimizes trend distortion artefacts and preserves common medium-to-low frequency variability at centennial and longer time scales.

We used a global 0.5° by 0.5° gridded network of the self-calibrating Palmer drought severity index (scPDSI, van der Schrier *et al* 2013) available on application from the British Atmospheric Data Centre (http://badc.nerc.ac.uk). The monthly scPDSI records from 1901 to 2012 were calculated using the Penman-Monteith method for potential evapotranspiration (PET) calculations rather than the traditional Thornthwaite method that can over-emphasize the effects of temperature on estimated PET, a concern raised by Sheffield *et al* (2012). For the ANZDA, a subset of 1375 scPDSI grid points was extracted from the global data set for our geographic area of interest (figure 1).

A nested point-by-point regression (PPR) method (Cook *et al* 2007, Cook *et al* 2010a, 2010b, Touchan *et al* 2011) was used to reconstruct austral summer (December, January, February; DJF) scPDSI over the ANZDA domain for the network of 177 tree-ring and coral sites. The focus on the summer window was chosen in order to highlight drought periods most likely to adversely affect plant growth and to be consistent with previous drought atlas studies (e.g. Cook *et al* 2010b). As pointed out by St George *et al* (2010) the monthly Palmer drought sensitivity index data is highly autocorrelated so a longer seasonal window is likely to be represented and requires further investigation in future work. A limited search radius is typically defined as part of the PPR approach to reconstruction (Cook *et al* 1999). However, Cook *et al* (1999, 2010b) have previously found evidence of long-range verification skill using tree-ring chronologies as far away as 2500 km from individual grid points (their figure B1). This longer-range teleconnection between tree-rings and climate typically occurred over North America in regions with relatively little topographic relief such as the Great Plains where coherent climate patterns tend to be larger than those in more mountainous regions.

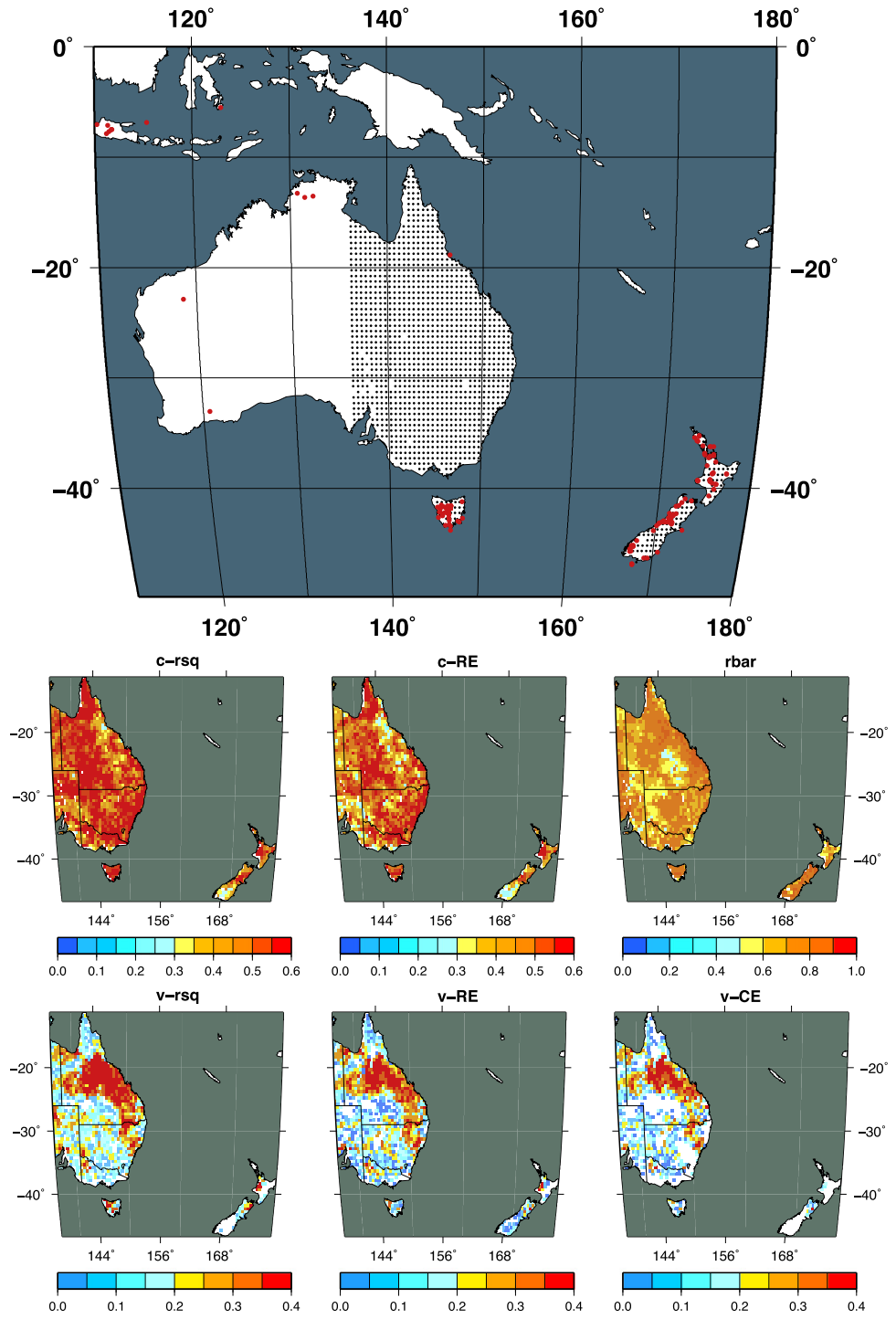


Figure 1. Location of the tree-ring and coral-proxy network and scPDSI grid-points (upper) along with the associated ensemble calibration/verification statistics (lower) for the 177 tree-ring and coral-proxy point-by-point regression to 1375 scPDSI indices for 0.5° grid-points covering Eastern Australia and New Zealand.

This expands the distance over which meaningful correlations between tree rings and climate can occur. The same should be expected in the Australian mainland that contains broad areas with relatively low topographic complexity, such as the Great Artesian Basin (1.7 million km^2, equivalent to 22% of Australia's total area) and the Murray–Darling Basin (1.1 million km^2, equivalent to 14% of Australia). In addition, much of these basin areas lack tree species suitable for dendroclimatology (i.e. lack distinct annual growth rings, or short-lived or frequently killed by fire). So to reconstruct scPDSI uniformly across the grid, it is necessary to 'bridge' these regions with estimates from tree-rings in neighbouring areas that usefully correlate with grid point scPDSI over these basin regions. Such bridging is always going to be necessary in some regions of Australia although future proxy record developments may enable the radius to

be reduced. Due to the large area involved and the lack of local chronologies for mainland Australia, we relaxed the search radius in this study to 4000 km. This relaxation of the search radius also enabled tree-ring chronologies from New Zealand to be screened for inclusion in the scPDSI reconstruction over Eastern Australia. The use of remote proxies to reconstruct local climate is a recognized concern because of potential instabilities in the teleconnections between the proxies and the climate being reconstructed (Neukom and Gergis 2012, Gallant *et al* 2013). Consequently we have limited our interpretations to large-scale features and related climate forcing.

Following standard statistical calibration and verification procedures used in dendroclimatology (Fritts 1976, Cook and Kairiukstis 1990), a split calibration/verification procedure was used to reconstruct the ANZDA and test it for validity. The last year of the calibration period was restricted to 1975 because several New Zealand chronologies were collected at that time and have not since been updated. The decision was therefore made to use the1930–1975 period for calibration and the 1902–1930 period for verification. This was done with and without autoregressive (AR) modelling of the tree-ring and climate variables and for eight different correlation weightings of the proxies (see Cook *et al* 2010b) resulting in 16 different model outputs.

As noted out in Cook *et al* (2010b) there is no *a priori* reason to select any particular weighting. Here we use the default of a zero weight and then seven additional values that span the range from 0.1 to 2.0 (i.e. 0.1, 0.25, 0.5, 0.67, 1.0, 1.5, 2.0). AR modelling is often used because many tree-ring series are positively autocorrelated in excess of the climate variable being reconstructed. This can introduce spectral bias in the reconstruction (Franke *et al* 2013) but, as described by Meko (1981) and Cook *et al* (1999), this problem can be ameliorated using appropriate time series modelling techniques such as AR modelling or by including lagged variables in regression. The 16 ANZDA ensemble members produced here were then averaged together, calibrated and verified again, and rescaled to recover lost variance due to the regression. The methods used are consistent with Cook *et al* (2010a, 2010b) so this means instrumental data has been appended to the reconstruction for the years after the 1930–1975 calibration period. The rescaling of the reconstructions, point by point over the calibration and verification periods, enables them to be directly blended with the instrumental data after 1975.

In addition to verification over the 1902–1930 instrumental period, we also examined the reliability of our reconstructed scPDSI by comparing the gridded reconstruction to historical records (Russell 1877) of summer climate conditions experienced by the first European settlers in New South Wales after landing in January 1788 (the 'first fleet'). Further comparisons were restricted to instrumental and other proxy records as local orographic influences and the observational quality of some records are thought to have resulted in the under-representation of wet phases in the documentary record (Gergis and Ashcroft 2012, Ashcroft *et al* 2015).

To characterize the main patterns of drought variability in the ANZDA since CE 1500, empirical orthogonal function analysis (EOF) was used. A range of comparisons using the ANZDA leading EOF mode (ANZDA-EOF1) were undertaken starting with a chi-square test (X^2) of normalized hydroclimate anomalies from a 45-station rainfall network located over the southeast Australian region (SEA, Gergis and Ashcroft 2012, table 1(a)). This included calculating a series of cross-correlations (1902–1975) between the ANZDA-EOF1 and climate indices (El Niño Southern Oscillation as the Niño 3.4 index, the interdecadal Pacific oscillation or IPO index and a tripole IPO index developed by Henley *et al* 2015), as well as other published proxies (Vance *et al* 2013, 2015, table 1(b)). Two tripole IPO indices developed by Henley *et al* (2015), the first based on the Hadley SST (HadlSST, Kennedy *et al* 2015) and the second on the extended and reconstructed SST (ERSST, Smith *et al* 2008 data, table 1(c)) were also used. Of the two tripole indices, the HadISST-based tripole index was more strongly correlated with instrumental and reconstructed scPDSI, so only these results are shown (DJF, figures 3(a) and (b)).

3. Results and discussion

3.1. Calibration and verification

The widely used statistical checks on the split-period calibration and verification regression results (Cook and Kairiukstis 1990) show that our climate field reconstruction is robust (figure 1). The Pearson squared-correlation values for verification (v-RSQ panel in figure 1) indicate a broad scale and highly positive association between instrumental and reconstructed scPDSI across eastern Australia and especially for Queensland. In New Zealand the pattern appears more restricted to the western North Island and northern South Island. These patterns persist with the reduction of error (RE, Fritts 1976) tests for calibration and verification (c-RE, v-RE; figure 1) and the more stringent coefficient of efficiency (CE) tests (Cook and Kairiukstis 1990).

An extensive area of grid-points across continental Australia, Tasmania and New Zealand were calibrated and verified. A large number of grid-points, particularly centred in Queensland, also passed the CE test. These results clearly demonstrate that the network of 177 proxy records successfully reconstructs scPDSI variability over eastern Australia and New Zealand despite the relative sparseness of proxy records over the region. The extensive geographic spread of the positive CE test results (figure 1) also demonstrates

Table 1. Eastern Australia and New Zealand Drought Atlas (ANZDA) reconstructed scPDSI comparisons to instrumental and proxy-climate records.

(a) Chi-square test (X^2) of normalized hydroclimate anomalies from the 45-station network over the Southeast Australian region (SEA, Gergis and Ashcroft 2012) to the ANZDA-EOF1 for 1860–2008. Each year, the SEA and ANZDA-EOF1 were ascribed an index value of 1 (wet), 0 (neutral) or −1 (dry) with the totals below indicating each of three possible outcomes (categories): *zero* when both index values have the same value (positive, negative or neutral), *One* when one value was neutral and the other was wet/dry, and finally, *Two* when the index values were opposite. Note, expected values have been rounded-up.

	Zero	*One*	*Two*	Total
Observed	77	61	11	149
Expected	50	66	33	149

$X^2_{(df = 2,\, N = 149)} = 31.7, p \ll 0.001\ (p = 1.268\text{e-}07)$

(b) Pearson RSQ cross-correlations (1902–1975) between climate indices (Nino34, IPO, TPI), published proxies (LDsss, PLF, DT, Vance *et al* 2013, 2015) and the leading EOF of the ANZDA.

	Nino34 (dJF)	IPO (dJF)	TPI (dJF)	LDsss	PLF	DT	ANZDA EOF1
Nino34(dJF)		0.728	0.846	0.131	0.011	0.015	**0.215**
IPO(dJF)			0.897	0.081	0.149	0.179	**0.370**
TPI(dJF)				0.106	0.063	0.084	**0.383**
LDsss	0.129	0.073	0.102		0.000	0.000	0.031
PLF	0.011	0.191	0.096			0.946	0.059
DT-median	0.016	0.225	0.124				0.092
ANZDA EOF1	**0.213**	**0.384**	**0.393**				
	Nino34 (dJFM)	IPO (Annual)	TPI (Annual)				

(c) Demonstration tests of the December–February tripole IPO signal in the leading EOF of the Australia-New Zealand Drought Atlas (ANZDA) using the HadISST and ERSST estimates of the tripole IPO index (Henley *et al* 2015) for split calibration and validation testing. All models successfully calibrated and validated, with the HadISST tripole IPO index producing the stronger results.

HadISST	Calibration Period			Validation Period Tests				
Model	FY	LY	RSQ	FY	LY	RSQ	RE	CE
Early	1871	1923	0.366	1924	1975	0.250	0.194	0.171
Late	1924	1975	0.250	1871	1923	0.366	0.315	0.298

Table 1. (Continued.)

ERSST	Calibration Period			Validation Period Tests				
Model	FY	LY	RSQ	FY	LY	RSQ	RE	CE
Early	1871	1923	0.280	1924	1975	0.144	0.090	0.090
Late	1924	1975	0.144	1871	1923	0.280	0.237	0.237

Key:
HadlSST—Hadley centre sea ice and sea surface temperature data set available from KNMI climate explorer (http://climexp.knmi.nl/).
ERSST—Extended reconstructed sea surface temperature (ERSST) data set available from KNMI climate explorer (http://climexp.knmi.nl/).
FY—First or initial year of calibration/verification.
LY—Last or final year of calibration/verification.
RSQ—Calibration or verification squared Pearson correlation.
RE—Reduction of error statistic.
CE—Coefficient of efficiency test.
Nino34—Nino 3.4 sea-surface temperatures produced by Kaplan *et al* (1998) and available from KNMI climate explorer (http://climexp.knmi.nl/).
IPO—Interdecadal Pacific oscillation; Power *et al* (1999), available from KNMI climate explorer (http://climexp.knmi.nl/).
TPI—Tripole index of the IPO, Henley *et al* (2015).
LDsss—Law Dome summer sea salt, Vance *et al* (2013).
PLF—Piecewise linear fit IPO reconstruction, Vance *et al* (2015).
DT—Decision tree IPO reconstruction, Vance *et al* (2015).
dJF—Austral summer months of December, January and February.
dJFMExtended austral summer of dJF and March.
Annual—An austral year starting in winter (June) and ending in autumn (May).

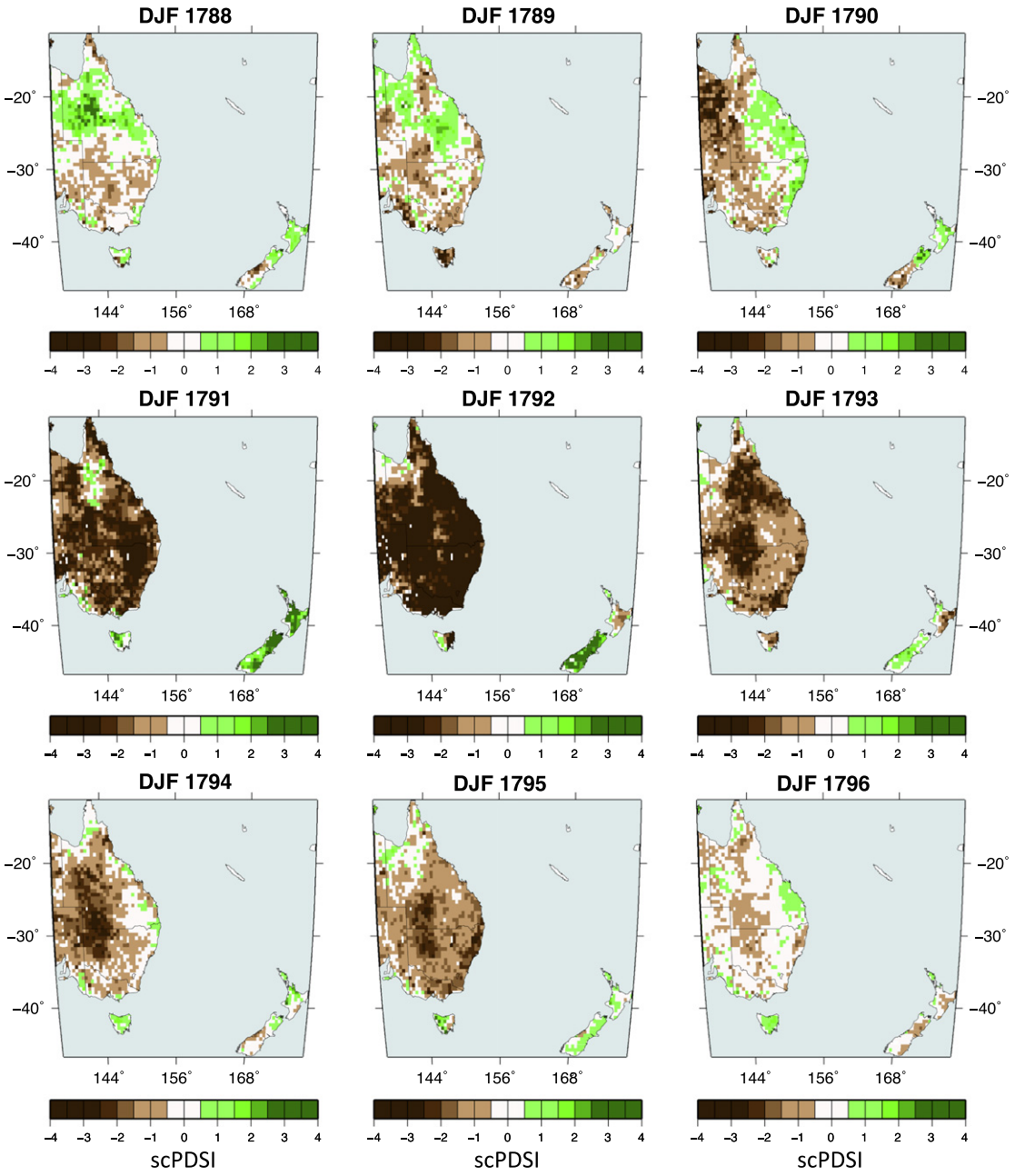


Figure 2. Reconstructed austral summer (December–February) scPDSI 0.5° grid-cells for the successive years of CE 1788–1796 during which the first European settlers landed in New South Wales in January 1788 and then recorded their experience of a drought starting in 1791–2 (Russell 1877).

that the relationships over the calibration and verification periods were stable.

One example of the reliability of the ANZDA scPDSI reconstruction is the clear detection of the 1791 to 1792 drought (the so-called 'settlement drought'; figure 2). Heavy rains in February 1790 are described in Russell (1877, p55) but then no rain fell at Sydney from June to November and the wheat harvest was a partial failure (Russell 1877, p56). During the following January and February of 1791 there were several weeks of excessive heat during which 'birds dropped dead from the trees, and almost every green thing was burnt up' (Russell 1877, p56). In November 1791 high temperatures and the dried-up water supply for Sydney resulted in some ships being sent out to collect water. By April 1793, Russell (1877, p58) reported that 'the rain of April came too late to save the Indian corn of the season, which now wore a most unpromising appearance'. More recent work by Gergis *et al* (2010) considers the drought conditions of 1791–93 to be associated with an El Niño event that is thought to have threatened the success of the First Fleet settlement and agricultural development in the nascent colony. The compilation of documentary sources by Fenby and Gergis (2012) and Gergis and Ashcroft (2012) lists 1790 and 1791 as dry years, and 1792 only as normal. This apparent anomaly can be explained by the fact that an 'annual' (i.e. January to December

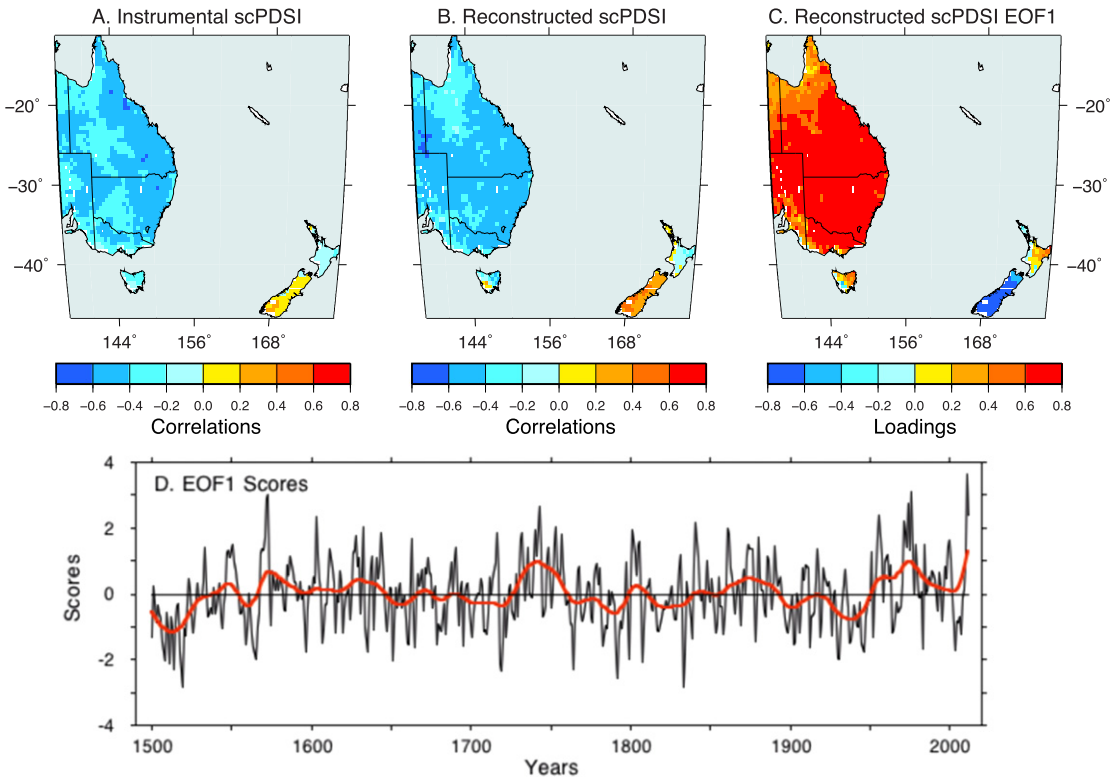


Figure 3. Comparisons of the IPO-tripole index (Henley *et al* 2015) for December–February calculated using HadlSST with instrumental scPDSI(a) and ANZDA reconstructed scPDSI(b) over the period 1902–1975. The first unrotated principal component (EOF1) from the full reconstructed period (i.e. 1500–1975) is shown in (c) with the fully extended scores plotted in (d) along with a 20-year spline (red line).

calendar year) record is reported by Fenby and Gergis (2012), whereas our reconstructed records describe the austral summer (December–February) that spans two calendar years. So, as noted by Russell (1877), the dry conditions in 1790 started after the summer, and in the case of 1792, we provide evidence of a summer drought prior to the arrival of the autumn rains that lead Fenby and Gergis (2012) to consider the 1792 calendar year as normal. Importantly, our results demonstrate this event was experienced across all of eastern Australia and was not restricted to the immediate Sydney region.

3.2. Regional driver(s) of hydroclimate

Recent efforts to compile and screen early instrumental and historical records have resulted in several papers exploring Southeast Australia's (SEA) hydroclimate and climate teleconnections (e.g. Ashcroft *et al* 2013, 2014, 2015). These studies all present caveats about interpretations based on the early historical data due to their geographical bias and reliability issues. As a result, subsequent investigations have primarily focused on the instrumental and proxy records. Here we address this apparent knowledge gap.

The leading EOF of the ANZDA scPDSI reconstruction since 1500 (ANZDA-EOF1) captures over 50% of the total variance in our gridded reconstructions and this was used for comparisons with other records (figures 3(c) and (d)), with a quasi-periodicity of ∼50 years. Comparison of ANZDA-EOF1 with the normalized hydroclimate anomalies from the 45-station Southeast Australian region (SEA, Gergis and Ashcroft 2012) for the period 1860–2008 showed a significant match (X^2 test, $p < 0.001$; table 1(a)). The very low level (7% or 11/149) of clear mismatches—where one variable was strongly positive and the other was strongly negative or vice-versa—indicates the fidelity of the ANZDA to the regional hydroclimatic record.

The ANZDA-EOF1 reconstruction (figure 3(d)) also clearly shows that the summer drought conditions during the Australian millennium drought (∼1997–2008) were not as severe as either the Federation drought (∼1895–1902) or the World War II drought (∼1937–1945). These three droughts had very different spatial signatures and magnitudes of impact (Verdon-Kidd and Kiem 2009) and this helps to explain why our results differ from the more localized interpretation of Gergis and Ashcroft (2013). The apparent capture of low frequency (multi-decadal) variations in our ANZDA-EOF1 reconstruction is important for comparisons of events and placing recent experiences in a historical context. For example, the wetter period during the 1950s to the 1970s seems to have only one other similar extended window from 1730 to 1760 (figure 3(d)) with important

implications for the allocation of water resources, including meeting sustainable agricultural needs.

Using a cross-correlation matrix for the period 1902–1975 we also compared ANZDA-EOF1 to a range of different climate indices and proxy records (table 1(b)). The three climate indices were the Nino 3.4 SST (Nino34, Kaplan *et al* 1998), the interdecadal Pacific oscillation (IPO, Power *et al* 1999) and the tripole index of the IPO (TPI, Henley *et al* 2015). The first proxy series was the summer sea-salt record from the summit of Law Dome (LDsss), east Antarctica (Vance *et al* 2013, 2015), which is significantly linked to ENSO and also with annual rainfall in eastern mainland Australia. The second and third proxy series were the IPO reconstructions produced by two independent non-linear multivariate regression techniques (piecewise linear fit and decision tree, Vance *et al* 2015). The results (table 1(b)) show that the ANZDA-EOF1 is significantly correlated with all of the instrumental climate indices (the strongest correlation being with the TPI) but not to any of the proxies. One potential contributing factor for the low correlation values might be the difference in seasonality recorded in the various indices and proxies. To further investigate this, the lower portion of table 1(b) includes the extended four-month summer used by Vance *et al* (2013) or the annual measures in Vance *et al* (2015). In both cases the strongest results were still obtained from the ANZDA-EOF1. Despite the largest correlation coefficient being between the annual TPI and the ANZDA-EOF1, we focused our reconstruction on the austral summer for consistency and potential comparisons with Northern Hemisphere drought atlases (e.g. Cook *et al* 2007, 2010b). The selection of summer is also important as this is typically the high season for plant growth making the atlas particularly relevant to agriculture.

Given the strength of the correlations between the ANZDA-EOF1 and instrumental climate indices (table 1(b)) we compared the spatial pattern of the relationship between the TPI and both the instrumental and reconstructed scPDSI series over the period 1902–1975 (figures 3(a) and (b)). The correlation patterns were very similar for the instrumental and reconstructed series with eastern Australia and the North Island of New Zealand being entirely negative (i.e. a dry (wet) summer correlates with a positive (negative) TPI and vice-versa). In contrast, the South Island and southwestern Tasmania had a positive correlation (i.e. a dry (wet) summer correlates with a negative (positive) TPI). To check the reliability of the response, conventional split calibration and validation testing of the summer TPI signal in the ANZDA-EOF1 using the HadISST and ERSST estimates of the TPI index was undertaken (table 1(c), Henley *et al* 2015). All models were successfully calibrated and validated, with the HadISST TPI producing the stronger results. Thus, there is an excellent basis for future reconstruction of the TPI and wider comparisons to proxy climate reconstructions.

We find a remarkable consistency between reconstructed scPDSI and the IPO phases identified by Henley *et al* (2015) between 1870 and 1976 (figure 4). Reconstructed scPDSI in eastern Australia was strongly and predominantly negative (drought) during the two positive IPO phases and positive (wet) during the two negative IPO phases (figure 4). During the most recent period (1977–2012) however, the relationship between the IPO and east Australian scPDSI is not as clear—negative and positive phases of the IPO show similar values of scPDSI. The reconstruction of scPDSI during this period (since 1975) was based entirely on instrumental scPDSI. Further investigation concerning this lack of distinction between positive and negative TPI phases for the most recent period is required. However, the more distinct earlier phases indicate the potential for screening for similar past positive and negative periods especially during the transition from the Little Ice Age (e.g. Cox and Jones 2008, Lorrey *et al* 2014).

Our analyses demonstrate a significant connection between ANZDA-EOF1 and the IPO (table 1(c), figure 4). Asymmetric modulation of ENSO events by the IPO has important impacts on east Australian precipitation (Verdon *et al* 2004), and McGowan *et al* (2009) have also shown that the low frequency oscillation of the IPO modulates annual flows into the headwaters of the Murray River. Furthermore, Gallant *et al* (2013) have noted non-stationary relationships between the southern annular mode, Niño 3.4 and precipitation over Australia on the 31–71 year timescale. A preliminary analysis of the spectral characteristics of the ANZDA-EOF1 using the multi-taper method with three 2-pi tapers for the identification of narrowband signals and a red noise significance test (Thomson 1982) revealed spectral peaks at ∼21 and 102 years, confirming the presence of multidecadal variability in the drought atlas (also seen in figure 2). Low frequency modulation of eastern Australia's hydroclimate presents particular challenges to the detection of an anthropogenically-driven trend in the occurrence of east Australian drought above background variability. By providing a multicentennial record of drought in eastern Australia that is linked to the IPO, the ANZDA offers a vital and unique long-term perspective on low-frequency drought variability. The ANZDA is therefore an essential tool for assessing anthropogenically-driven changes in drought frequency, length and severity.

4. Conclusions

Our network of tree-ring and coral records has successfully reconstructed a 0.5° gridded drought atlas for eastern Australia and New Zealand since CE 1500 —the first such drought atlas for the SH. The ANZDA

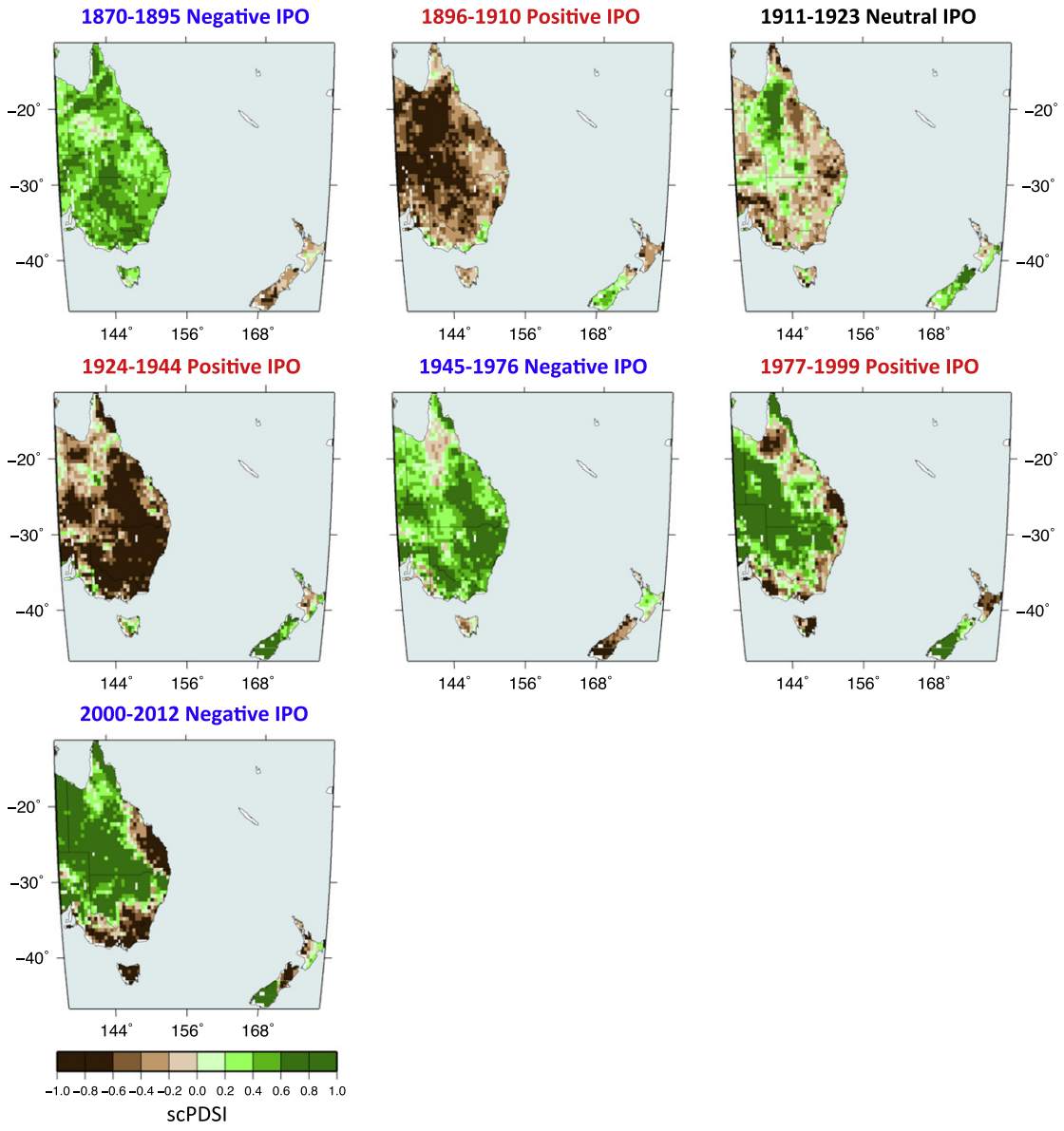


Figure 4. Maps of DJF ANZDA drought and wetness averaged over the IPO phases defined in figure 5 of Henley *et al* (2015). Maps up to 1976 are, except for the 1976 datum, based solely on tree-ring estimates of scPDSI. Those after 1976 are based on instrumental scPDSI.

not only reproduced the oldest known extreme drought in the historical record that directly impacted on the first European settlers in New South Wales in CE 1791–2, but provides a broader spatial context for the scale and intensity of that drought across eastern Australia. The comparison with a compilation of 45 instrumental rainfall records from southeast Australia extending from CE 1860 was highly significant. Principal components analysis highlighted the large amount of common variance accounted for by the ANZDA. Confidence in the robustness of the ANZDA was further enhanced by the strong positive relationships with climate indices known to modulate the regional climate. The strongest correlations were with the tripole index of the IPO and modelling calibration/verification tests showed the scope for reconstruction of this index back to CE 1500. Overall the results also demonstrate the potential of the ANZDA to overcome a common limitation in hydroclimatic risk assessment by providing a long record with which to assess decadal to multidecadal variability. Finally, the production of the ANZDA highlights the need for extending existing records (both further back in time and forward to the present day) as well as increasing the spatial coverage of the proxy network.

Acknowledgments

Support was provided by the Australian Research Council through grants: FL100100195, LP120100310 and DP130104156 for CSMT and DP0878744, DP120104320, LP120200811, FT120100715 for PJB, Lamont-Doherty Earth Observatory Contribution No. 7948.

References

Ashcroft L, Gergis J and Karoly D J 2014 A historical climate dataset for Southeastern Australia, 1788–1859 *Geosci. Data J.* **1** 158–78

Ashcroft L, Gergis J and Karoly D J 2015 Long-term stationarity of El Niño–Southern Oscillation teleconnections in Southeastern Australia *Clim. Dyn.* in press (doi:10.1007/s00382-015-2746-3)

Ashcroft L, Karoly D J and Gergis J 2013 Southeastern Australian climate variability 1860–2009: a multivariate analysis *Int. J. Climatol.* **34** 1928–44

Bell A R, Osgood D E, Cook B I and Anchukaitis K J 2013 Paleoclimate histories improve access and sustainability in index insurance programs *Glob. Environ. Change* **23** 774–81

Cook E R and Kairiukstis L A (ed) 1990 *Methods of dendrochronology —Applications in the Environmental Sciences* (The Netherlands: Kluwer)

Cook E R, Seager R, Heim R R, Vose R S, Herweijer C and Woodhouse C 2010a Megadroughts in North America: placing IPCC projections of hydroclimatic change in a long-term palaeoclimate context *J. Quat. Sci.* **25** 48–61

Cook E R, Anchukaitis K J, Buckley B M, D'Arrigo R D, Jacoby J C and Wright W E 2010b Asian monsoon failure and megadrought during the last millennium *Science* **328** 486–89

Cook E R, Meko D M, Stahle D W and Cleaveland M K 1999 Drought reconstructions for the continental United States *J. Clim.* **12** 1145–62

Cook E R, Seager R, Cane M A and Stahle D W 2007 North American drought: reconstructions, causes, and consequences *Earth–Sci. Rev.* **81** 93–134

Cox P and Jones C 2008 Climate change, illuminating the modern dance of climate and CO_2 *Science* **321** 1642–44

Cullen L E and Grierson P F 2009 Multi-decadal scale variability in autumn–winter rainfall in south-western Australia since 1655 AD as reconstructed from tree rings of Callitris columellaris *Clim. Dyn.* **33** 433–44

Ding Y, Hayes M J and Widhalm M 2011 Measuring economic impacts of drought: a review and discussion *Disaster Prevention Manage.* **20** 434–46

Enright N and Ogden J 1995 *Ecology of the Southern Conifers* (Melbourne: Melbourne University Press)

Fenby C and Gergis J 2012 Rainfall variations in South-eastern Australia: I. Consolidating evidence from pre-instrumental documentary sources, 1788–1860 *Int. J. Climatol.* **33** 2956–72

Franke J, Frank D, Raible C C, Esper J and Brönnimann S 2013 Spectral biases in tree-ring climate proxies *Nat. Clim. Change* **3** 360–64

Fritts H C 1976 *Tree Rings and Climate* (London: Academic)

Gallant A J E, Phipps S J, Karoly D J, Mullan A B and Lorrey A M 2013 Nonstationary Australasian teleconnections and implications for paleoclimate reconstructions *J. Clim.* **26** 8827–49

Gergis J and Ashcroft L 2012 Rainfall variations in South-eastern Australia : II. A comparison of documentary, early instrumental and palaeoclimate records, 1788–2008 *Int. J. Climatol.* **33** 2973–87

Gergis J, Garden D and Fenby C 2010 The influence of climate on the first European settlement of Australia: a comparison of weather journals, documentary data and palaeoclimate records, 1788–1793 *Environ. Hist.* **15** 485–507

Grissino-Mayer H D 2001 Evaluating crossdating accuracy: a manual and tutorial for the computer program COFECHA *Tree-Ring Res.* **57** 205–21

Heinrich I and Allen K 2013 Current issues and recent advances in Australian dendrochronology: where to next? *Geogr. Res.* **51** 180–91

Henley B J, Gergis J, Karoly D J, Power S, Kennedy J and Folland C K 2015 A tripole index for the interdecadal Pacific oscillation *Clim. Dyn.* in press (doi:10.1007/s00382-015-2525-1)

Holmes R L 1983 Computer-assisted quality control in tree-ring dating and measurement *Tree-Ring Bull.* **43** 69–78

Horridge M, Madden J and Wittwer G 2005 The impact of the 2002–2003 drought on Australia *J. Policy Model.* **27** 285–308

Kaplan A, Cane M, Kushnir Y, Clement A, Blumenthal M and Rajagopalan B 1998 Analyses of global sea surface temperature 1856–1991 *J. Geophys. Res.* **103** 18567–589

Kennedy J J, Rayner N A, Millington S C and Saunby M 2015 The Met Office Hadley Centre sea ice and sea-surface temperature data set, Version 2: 2 *Sea-Surface Temp. Anal.* in preparation

Kiem A S, Franks S W and Kuczera G 2003 Multi-decadal variability of flood risk *Geophys. Res. Lett.* **30** 1035

LaMarche V C, Holmes R L, Dunwiddie P W and Drew L G 1979 *Tree–ring chronologies of the Southern Hemisphere, Chronology Series V* (Tucson: Laboratory of Tree–ring Research, University of Arizona)

Lorrey A, Fauchereau N, Stanton C, Chappell P, Phipps S, Mackintosh A, Renwick J, Goodwin I and Fowler A 2014 The Little Ice Age climate of New Zealand reconstructed from Southern Alps cirque glaciers: a synoptic type approach *Clim. Dyn.* **42** 3039–60

McDonald C 2013 Drying out: Investigating the economic effects of drought in New Zealand *Reserve Bank of New Zealand Analytical Note Series* pp 1–31

McDougall K L, Brookhouse M T and Broome L S 2012 Dendroclimatological investigation of mainland Australia's only alpine conifer, Podocarpus lawrencei Hook.F *Dendrochronologia* **30** 1–9

McGowan H, Samuel A, Marx K, Denholm J, Soderholm J and Kamber B S 2009 Reconstructing annual inflows to the headwater catchments of the Murray River, Australia, using the Pacific decadal oscillation *Geophys. Res. Lett.* **36** L06707–5

Meko D M 1981 Applications of Box-Jenkins methods of time series Analysis to the reconstruction of drought from tree rings *PhD Dissertation* The University of Arizona, Arizona p 149

Melvin T M and Briffa K R 2008 A 'signal-free' approach to dendroclimatic standardisation *Dendrochronologia* **26** 71–86

Neukom R and Gergis J 2012 Southern Hemisphere high-resolution palaeoclimate records of the last 2000 years *Holocene* **22** 501–24

O'Donnell A J, Cook E R, Palmer J G, Turney C S M, Page G F M and Grierson P F 2015 Tree rings show recent high summer-autumn precipitation in Northwest Australia is unprecedented within the last two centuries *PLoS One* **10** e0128533

Power S, Casey T, Folland C, Colman A and Mehta V 1999 Inter-decadal modulation of the impact of ENSO on Australia *Clim. Dyn.* **15** 319–24

Power S, Tseitkin F, Torok S and Lavery B 1998 Australian temperature, Australian rainfall and the Southern Oscillation, 1910–1992: coherent variability and recent changes *Aust. Meteorol. Mag.* **47** 85–101

Russell H C 1877 *Climate of New South Wales: Descriptive, Historical and Tabular* (Sydney: C. Potter for Government Printer) p 252

Sheffield J, Wood E F and Roderick M L 2012 Little change in global drought over the past 60 years *Nature* **491** 435–38

Smith T M, Reynolds R W, Peterson T C and Lawrimore J 2008 Improvements NOAAs historical merged land–ocean temp analysis (1880–2006) *J. Clim.* **21** 2283–96

St George S, Meko D M and Cook E R 2010 The seasonality of precipitation signals embedded within the North American Drought Atlas *Holocene* **20** 983–88

Thomson D J 1982 Spectrum estimation and harmonic analysis *Proc. IEEE* **70** 1055–96

Touchan R, Anchukaitis K J, Meko D M, Sabir M, Attalah S and Aloui A 2011 Spatiotemporal drought variability in Northwestern Africa over the last nine centuries *Clim. Dyn.* **37** 237–52

Vance T R, Roberts J L, Plummer C T, Kiem A S and van Ommen T D 2015 Interdecadal Pacific variability and Eastern Australian megadroughts over the last millennium *Geophys. Res. Lett.* **42** 129–37

Vance T R, van Ommen T D, Curran M A J, Plummer C T and Moy A D 2013 A millennial proxy record of ENSO and Eastern Australian rainfall from the Law Dome ice core, East Antarctica *J. Clim.* **26** 710–25

van der Schrier G, Barichivich J, Briffa K R and Jones P D 2013 A scPDSI-based global data set of dry and wet spells for 1901–2009 *J. Geophys. Res.: Atmos.* **118** 4025–48

Verdon D C, Wyatt A M, Kiem A S and Franks S W 2004 Multidecadal variability of rainfall and streamflow: Eastern Australia *Water Resour. Res.* **40** W10201

Verdon-Kidd D C and Kiem A S 2009 Nature and causes of protracted droughts in Southeast Australia: comparison between the Federation, WWII, and Big Dry Droughts *Geophys. Res. Lett.* **36** L22707